temperature do not have any chemical bond with TiO_2 support and can easily move around, aided by their small sizes. As a result, the size grows with reduction temperature.

Conclusion

It is clear from the analysis of EXAFS that different oxides with various sizes are formed depending on the preparation method and on the calcination temperature. The structure of TiO_2 supported Co catalyst, which is prepared by reducing the oxides, strongly depends on the type and size of the oxides. Very small clusters of oxides are formed in the preparation by the alkoxide method at the calcination stage, which makes the size of metal particles of the reduced catalyst small and homogeneous. These conclusions are in very good accordance with those obtained previously for the Ni/SiO_2 catalyst.

Registry No. Co, 7440-48-4; TiO_2, 13463-67-7; Co_3O_4, 1308-06-1; $CoTiO_3$, 12017-01-5.

Carbene Complexes of Zirconium. Synthesis, Structure, and Reactivity with Carbon Monoxide To Afford Coordinated Ketene

Paul T. Barger, Bernard D. Santarsiero, Justine Armantrout, and John E. Bercaw*

Contribution No. 6835 from the Arthur Amos Noyes Laboratory of Chemical Physics, California Institute of Technology, Pasadena, California 91125. *Received July 5, 1983*

Abstract: Treatment of $Cp_2Zr(L)(CO)$ ($Cp = C_5H_5$; L = PMe_3, CO) with $Cp^*_2ZrH_2$ ($Cp^* = C_5Me_5$) affords zirconium oxycarbene complexes, $Cp_2(L)Zr{=}CHO{-}Zr(X)Cp^*_2$ (L = PMe_3, X = H, I; L = CO, X = H), that represent some of the first examples of group 4 metal-to-carbon multiple bonding. The first X-ray diffraction structure determination of a zirconium carbene complex, that of $Cp(PMe_3)Zr{=}CHO{-}Zr(I)Cp^*_2{\cdot}C_6H_6$, is reported ($C2/c$, a = 27.318 (4) Å, b = 19.895 (3) Å, c = 19.932 (5) Å β = 132.188 (10)°, Z = 8) and shows a very short Zr-C bond length of 2.117 (7) Å. Treatment of $Cp_2(CO)Zr{=}CHO{-}Zr(H)Cp^*_2$ with CH_3I or $Cp_2(PMe_3)Zr{=}CHO{-}Zr(I)Cp^*_2$ with CO affords the zirconium substituted enediolate zirconacycle, $Cp^*_2ZrOCH{=}C(Zr(I)Cp_2)O$, which has been characterized by an X-ray diffraction study ($P2_1/c$, a = 15.866 (4) Å, b = 10.673 (3) Å, c = 20.561 (4) Å, β = 105.5 (2)°, Z = 4). It is proposed that this complex forms by coupling of the zirconoxycarbene and a carbonyl to give a metal-coordinated ketene intermediate that subsequently rearranges to the isolated product. An isotopic crossover experiment has demonstrated that the new carbon-carbon bond is formed in an intramolecular coupling step. The ketene intermediate can be trapped by dissolving $Cp_2(CO)Zr{=}CHO{-}Zr(H)Cp^*_2$ in pyridine, giving $Cp_2(py)Zr(O{=}C{=}CHOZr(H)Cp^*_2)$. Treatment of the isolated ketene complex with CH_3I in benzene gives the enediolate zirconocycle; in pyridine $Cp_2(py)Zr(O{=}C{=}CHOZr(I)Cp^*_2)$ can be observed spectroscopically.

Bis(pentamethylcyclopentadienyl)zirconium hydrides have proven to be useful reagents for the reduction of transition-metal-bound carbon monoxide.[1-3] Previous work has demonstrated that these hydrides, in particular $Cp^*_2ZrH_2$ ($Cp^* = \eta^5$-C_5Me_5), can add across the carbon-oxygen bond of a carbonyl on a variety of metals to afford a zirconoxycarbene product (eq 1) or may lead to reductive elimination of H_2 and rearrangement

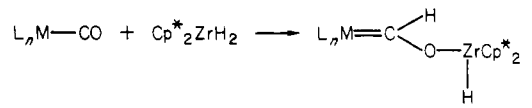

(1)

to afford carbonyl-bridged "early" and "late" mixed-metal dimers.[4,5] By the former reaction pathway oxycarbene complexes of niobium,[2] chromium,[3] molybdenum,[3] tungsten,[3] cobalt,[5] and rhodium[5] have been prepared. $Cp^*_2ZrH_2$ also appears to add readily to iron and ruthenium carbonyls,[5] but the carbenes prepared have proven unstable toward further rearrangement.

The first indication that $Cp^*_2ZrH_2$ could reduce carbon monoxide bound to zirconium was the preparation of *cis*-$(Cp^*_2ZrH)_2(\mu$-$OCH{=}CHO{-})$ by the treatment of $Cp^*_2Zr(CO)_2$ with $Cp^*_2ZrH_2$ under an H_2 atmosphere,[1,3]

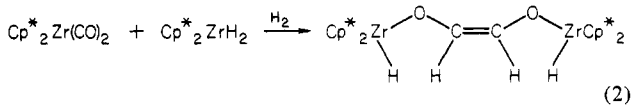

(2)

the proposed mechanism[1d] of which is shown in Scheme I. Some aspects of this mechanism have now been tested by preparing models for the proposed intermediates and examining their reactivity.

The initial step of Scheme I is the formation of a zirconoxycarbene of complex of zirconium, similar to those isolated for group 5 and 6 transition metals. Without H_2, $Cp^*_2Zr(CO)_2$ and $Cp^*_2ZrH_2$ give a myriad of products, involving a number of transient species. The instability of the intermediate(s) is presumably due to two factors: (1) unfavorable steric interactions of the bulky decamethylzirconocene fragments forced into close contact by the small, two-atom zirconoxycarbene bridge and (2) the presence of an adjacent carbonyl ligand, which may allow for facile decomposition pathways. In our efforts to prepare stable zirconium zirconoxycarbene complexes, these factors have been taken into account.

The only previous reports of carbene complexes of zirconium have been by Schwartz and co-workers. In 1980 the spectroscopic observation of $Cp_2Zr(CH_2)(PPh_2Me)$ was reported, although

$$Cp_2Zr(PPh_2Me)_2 + CH_2{=}PPh_3 \rightarrow Cp_2Zr(CH_2)(PPh_2Me) + PPh_3 + PPh_2Me \quad (3)$$

isolation of the product was prevented by its instability at room temperature under the reaction conditions.[6] More recently, Schwartz has reported the isolation of $Cp_2(L)Zr{=}C(H)(CH_2R)$ (L = PPh_3, PMe_2Ph; R = *t*-Bu, C_6H_{11}, CH(Me)(Et)) as impure oils.[7]

(1) (a) Manriquez, J. M.; McAlister, D. R.; Sanner, R. D.; Bercaw, J. E. *J. Am. Chem. Soc.* **1976**, *98*, 6733. (b) Manriquez, J. M.; McAlister, D. R.; Sanner, R. D.; Bercaw, J. E. *Ibid.* **1978**, *100*, 2716. (c) Bercaw, J. E. *Adv. Chem. Ser.* **1978**, *No. 167*, 136. (d) Wolczanski, P. T.; Bercaw, J. E. *Acc. Chem. Res.* **1980**, *13*, 121.
(2) Threlkel, R. S.; Bercaw, J. E. *J. Am. Chem. Soc.* **1981**, *103*, 2650.
(3) Wolczanski, P. T.; Threlkel, R. S.; Bercaw, J. E. *J. Am. Chem. Soc.* **1979**, *101*, 218.
(4) Barger, P. T.; Bercaw, J. E. *J. Organomet. Chem.* **1980**, *201*, C39.
(5) Barger, P. T.; Bercaw, J. E. *Organometallics*, **1984**, *3*, 278-284.

0002-7863/84/1506-5178$01.50/0

Scheme I

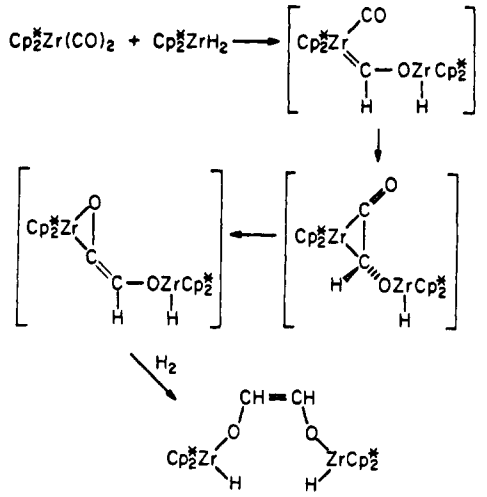

The second step proposed in Scheme I, an intramolecular coupling of the carbene and carbonyl ligands to give a metal ketene intermediate, is an important step in organometallic chemistry which warrants further study.[8] The use of transition metals to catalyze the formation of new C–C bonds is an important part of industrial processes which use CO as a feedstock for products with more than one carbon atom. Commonly invoked mechanisms for metal-catalyzed C–C bond making include carbonyl insertion[9,10] (hydroformylation and methanol carbonylation) and polymerization of surface methylene (derived from CO and H_2) on metal surfaces to give linear hydrocarbons[11] in Fischer–Tropsch synthesis. The possibility of carbene–carbonyl coupling to give new C–C bonds has received much less attention. In 1960 Schrauzer and Rüchardt reported that in the presence of $Ni(CO)_4$ diazomethanes give products which presumably arise from a nickel carbene carbonyl intermediate that releases a substituted ketene (which was trapped with ethanol) upon decomposition.[12] Carbonylation of $(CO)_5Cr{=}C(OMe)Ph$[13] (150 atm of CO) or $Cp_2Mo_2(CO)_4(\mu\text{-}CR_2)$[14] (R = C_6H_5, 3 atm of CO, 50 °C) also yields the corresponding ketene. The preparation of tantalum[15] and osmium[16] ketene complexes by carbonylation of a metal carbene have been briefly reported. Beauchamp and Stevens have proposed that $CpFe(CO)(CH_2)^+$, observed by ion cyclotron resonance spectroscopy, is best formulated as the iron ketene adduct, $CpFe(OCCH_2)^+$.[17] The most thoroughly examined system showing this type of reactivity to date has been reported by Herrmann and Plank for the high-pressure (650 atm) carbonylation of $CpMn(CO)_2(CPh_2)$ to afford $CpMn(CO)_2(OCCPh_2)$.[18a] Further studies of the less stable manganese anthronyl carbene complex, in the presence of $CpMn(CO)_3$, have suggested that the ketene product is formed by the intermolecular transfer of the carbene to one of the carbonyls of $CpMn(CO)_3$.[18b] Clear precedence for the *intra*molecular carbene–carbonyl coupling step proposed in Scheme I is clearly desirable, however.

In this paper we report the preparation of some stable zirconium zirconoxycarbene complexes by the reaction of $Cp^*_2ZrH_2$ with a bis(cyclopentadienyl)(trimethylphosphine)zirconium monocarbonyl complex, a less sterically hindered zirconium carbonyl than $Cp^*_2Zr(CO)_2$. We have also investigated the reactivity of a zirconoxycarbene–carbonyl complex of zirconocene, which undergoes facile, unimolecular carbene–carbonyl coupling to afford a metal-coordinated ketene complex.

Results

The treatment of $Cp_2Zr(L)(CO)$ (**1**, L = CO; **2**, L = PMe_3) with $Cp^*_2ZrH_2$ (**3**) in toluene gives an immediate reaction at −78 °C to afford the corresponding zirconoxy carbenes, $Cp_2(L)Zr{=}CHO{-}Zr(H)Cp^*_2$ (**4**, L = PMe_3; **5**, L = CO). In the case of

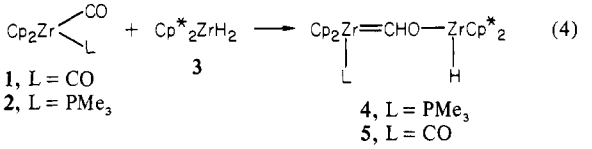

(4)

L = PMe_3, **4** is quite stable in solution and can be isolated as red crystals in 84% yield based on **3** from toluene/petroleum ether solution. The ^1H and ^{13}C NMR spectra of **4** (Table I) are similar to those of previously reported zirconoxy carbenes, $Cp_2M{=}CHO{-}Zr(H)Cp^*_2$ (M Cr, Mo, W)[3] and $Cp(R)Nb{=}CHO{-}Zr(H)Cp^*_2$ (R = H, CH_3, $CH_2C_6H_5$, $CH_2C_6H_4OCH_3$).[2] The carbene carbon and proton resonances appear at low field, δ 287.5 and 11.2, with $^1J_{CH}$ = 115 Hz. Two resonances are observed in the ^1H NMR spectrum for the C_5H_5 rings, presumably due to the restricted rotation around the zirconium–carbon bond. The π-interaction of the carbon p-orbital and the zirconium $1a_1$ orbital in the equatorial wedge of the Cp_2Zr metallocene fragment locks the carbene ligand with the proton directed toward one ring and the zirconoxy substituent toward the other. The lack of rotation of the carbene also makes the Cp* rings diastereotopic, as indicated by the inequivalent resonance signals in the ^1H and ^{13}C (methyl carbons only) NMR spectra. The zirconium hydride resonance at δ 5.7 is characteristic of compounds that have an adjacent zirconium–oxygen bond.

In contrast to **4**, **5** is unstable in solution at room temperature. However, $Cp_2(CO)Zr{=}CHO{-}Zr(H)Cp^*_2$ can be isolated as a tan powder in 53% yield by performing the reaction in petroleum ether, whereupon the slightly soluble carbene complex precipitates from solution as it is formed. The ^1H and ^{13}C NMR spectra of **5** (Table I) are similar to those of **4**. The zirconium carbonyl exhibits a strong band at 1925 cm^{-1} in the IR spectrum and is assigned as the ν_{CO}. Treatment of **5** with ca. 3 equiv of PMe_3 in a sealed NMR tube results in conversion to **4** within 2 h at 25 °C.

In toluene or benzene solution **5** converts to a very insoluble yellow crystalline compound (**6**) within 2 h at room temperature. The IR spectrum of this product shows no bands corresponding to a metal–carbonyl stretch; the elemental analysis of **6** indicates the same stoichiometry as **5**, $(Cp_2Zr)(Cp^*_2ZrH)(C_2HO_2)$ (see below).

Treatment of **4** with an excess of CH_3I liberates 1 equiv of CH_4 and yields green, crystalline $Cp_2(PMe_3)Zr{=}CHO{-}Zr(I)Cp^*_2$ (**7**). The ^1H and ^{13}C NMR spectra of **7** (Table I) are very similar

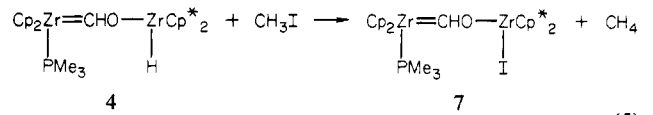

(5)

to those of **4**. In the presence of HCl **7** rapidly gives Cp_2ZrCl_2 and $Cp^*_2Zr(OCH_3)I$.

(6) Schwartz, J.; Gell, K. I. *J. Organomet. Chem.* **1980**, *184*, C1.
(7) Hartner, F. W.; Schwartz, J.; Clift, S. M. *J. Am. Chem. Soc.* **1983**, *105*, 641.
(8) Moloy, K. G.; Marks, T. J. *J. Am. Chem. Soc.* **1983**, *105*, 5696 and references cited therein.
(9) (a) Heck, R. F.; Breslow, D. S. *J. Am. Chem. Soc.* **1961**, *83*, 4023. (b) Calderazzo, F. *Angew. Chem., Int. Ed. Engl.* **1977**, *16*, 299.
(10) Forster, D. *Adv. Organomet. Chem.* **1979**, *17*, 255 and references cited therein.
(11) (a) Fischer, F.; Tropsch, H. *Brennst.-Chem.* **1926**, *7*, 97; *Chem. Ber.* **1926**, *59*, 830. (b) Brady, R. C., III; Pettit, R. J. *J. Am. Chem. Soc.* **1980**, *102*, 6181; *Ibid.* **1981**, *103*, 1287.
(12) Rüchardt, C.; Schrauzer, G. N. *Chem. Ber.* **1960**, *103*, 1287.
(13) Dorrer, B.; Fischer, E. O. *Chem. Ber.* **1974**, *107*, 2683.
(14) Messerle, L.; Curtis, M. D *J. Am. Chem. Soc.* **1980**, *102*, 7791.
(15) Messerle, L. Ph.D. Thesis, Massachusetts Institute of Technology, 1979.
(16) Roper, W. R. "Abstracts of Papers", 184th National Meeting of the American Chemical Society, Kansas City, MO, Sept 5–108 1982; American Chemical Society: Washington, D.C., 1982; INOR002.
(17) Stevens, A. E.; Beauchamp, J. L. *J. Am. Chem. Soc.* **1978**, *100*, 2584.
(18) (a) Herrmann, W. A.; Plank, J. *Angew. Chem., Int. Ed. Engl.* **1978**, *17*, 525. (b) Herrmann, W. A.; Plank, J.; Ziegler, M. L.; Wedenhammer, K. *J. Am. Chem. Soc.* **1979**, *101*, 3133.

Table I. NMR[a] and IR[b] Data

compd	IR		NMR assignment	^{1}H		^{13}C{^{1}H}	
$Cp_2(PMe_3)Zr{=}CHO{-}Zr(H)Cp^*_2$ (**4**)	ν(C–H)	2755	Zr=*CHO*–Zr	11.29	$^3J_{PH}$ = 3	287.5	$^1J_{CH}$ = 115, $^2J_{CP}$ = 14
	ν(C–D)	2045	C_5H_5	5.35, 5.44	$^3J_{PH}$ = 2, 2	100.2, 101.6	
			$C_5(CH_3)_5$	2.00, 2.04		11.8, 12.2	
			$C_5(CH_3)_5$			116.7	
			$P(CH_3)_3$	0.93	$^2J_{PH}$ = 6	20.3	$^1J_{CP}$ = 18
			Zr*H*	5.70			
$Cp_2(CO)Zr{=}CHO{-}Zr(H)Cp^*_2$ (**5**)[c]	ν(C–H)	2755	Zr=*CHO*–Zr	11.58		295.0	$^1J_{CH}$ = 105
	ν(C–D)	2042	C_5H_5	5.44, 5.43		98.6, 100.3	$^1J_{CH}$ = 172, 176
	ν(CO)	1925	$C_5(CH_3)_5$	1.95, 1.93		11.6	$^1J_{CH}$ = 127
	ν(Zr–H)	1515	$C_5(CH_3)_5$			116.2	
			Zr*H*	5.47		262.1	
$Cp_2(PMe_3)Zr{=}CHO{-}Zr(I)Cp^*_2$ (**7**)	ν(C–H)	2725	Zr=*CHO*–Zr	10.69	$^3J_{PH}$ = 4	286.3	$^1J_{CH}$ = 117, $^2J_{CP}$ = 14
	ν(C–D)	2020	C_5H_5	5.48, 5.55	$^3J_{PH}$ = 2, 2		
			$C_5(CH_3)_5$	2.07, 2.13			
			$P(CH_3)_3$	0.93	$^2J_{PH}$ = 6		
$Cp^*_2ZrOCH{=}C(Zr(I)Cp_2)O$ (**8**)			ZrO*CH*=C(Zr)O	6.77		155.0	$^1J_{CH}$ = 180, $^1J_{CC}$ = 45
			ZrOCH=*C*(Zr)O			235.0	$^2J_{CH}$ = 24
			C_5H_5	6.07		111.0	
			$C_5(CH_3)_5$	1.87		11.2	
			$C_5(CH_3)_5$			not assigned	
$Cp_2(pyr)Zr(O{=}C{=}CHO{-}Zr(H)Cp^*_2$ (**9**)[d]			O=*C*=CHO–Zr			165.7	$^2J_{CH}$ = 22, $^1J_{CC}$ = 77
			O=C=*CH*O–Zr	6.20		123.4	$^1J_{CH}$ = 183
			C_5H_5	5.91		107.5	$^1J_{CH}$ = 170
			$C_5(CH_3)_5$	2.20		11.7	$^1J_{CH}$ = 126
			$C_5(CH_3)_5$			116.9	
			Zr*H*	5.92			
$Cp_2(pyr)Zr(O{=}C{=}CHO{-}Zr(I)Cp^*_2)$ (**10**)[d]			O=*C*=CHO–Zr			170.8	$^1J_{CC}$ = 73
			O=C=*CH*O–Zr	6.28		124.4	
			C_5H_5	5.96		108.2	
			$C_5(CH_3)_5$	1.77		11.1	
			$C_5(CH_3)_5$			114.6	

[a] NMR spectra in benzene-d_6 at 34 °C at 90 MHz (^{1}H) or 22.5 MHz (^{13}C) unless otherwise noted. Chemical shifts in δ measured from internal Me_4Si, coupling constants in Hz. All ^{13}C NMR samples were enriched with ^{13}C at the non-ring and non-phosphine carbons. [b] IR spectra recorded as Nujol mulls. Values given in cm^{-1}. Detailed spectra are listed in the Experimental Section. [c] ^{1}H NMR spectrum recorded at 500 MHz. [d] Spectra recorded in pyridine-d_5.

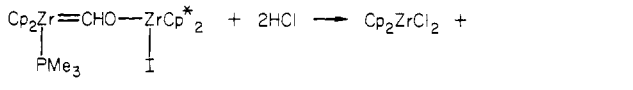

7

$$Cp^*_2Zr(OCH_3)I + PMe_3 \qquad (6)$$

Crystals of **7** suitable for X-ray diffraction were grown by slow cooling of a saturated benzene solution. The unit cell parameters and a summary of data collection and refinement information are given in Table II; atom coordinates are given in Table III.

Figure 1 indicates the important structural features of **7**. Both zirconium atoms have the pseudotetrahedral coordination geometries common for bent metallocene complexes (Figure 2). Cp and Cp* ligands are coordinated in the conventional η^5 manner to the metals with normal Zr–C and C–C bond lengths (Table VIII). The ring centroid–metal–ring centroid angles of 135.4° and 134.0° for the Cp_2Zr and Cp^*_2Zr fragments are reasonable for bent zirconocenes.[19] The Zr(2)–C(carbene) distance of 2.117 (7) Å is the shortest reported zirconium–carbon bond, being ca. 0.15 Å shorter than that observed for carbon σ-bonded to a zirconium center (these values range from 2.25 Å for (indenyl)$_2ZrMe_2$[20] to 2.33 Å for $Cp_2Zr(Ph)CH(SiMe_3)_2$).[21] When

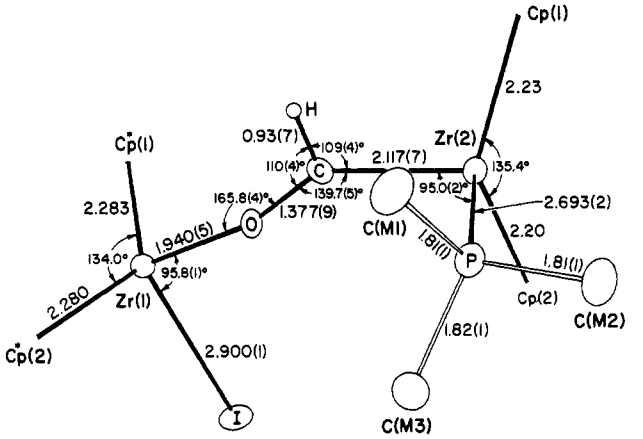

Figure 1. ORTEP drawing of **7** with important bond lengths and angles.

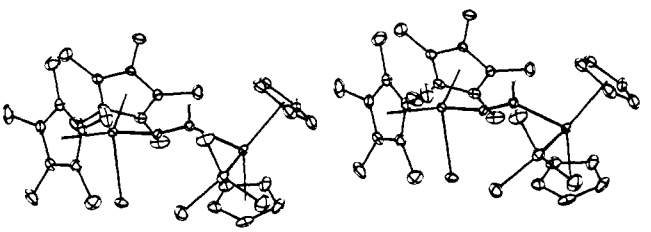

Figure 2. Stereoview of **7**.

(19) (a) Sanner, R. D.; Manriquez, J. M.; Marsh, R. E.; Bercaw, J. E. *J. Am. Chem. Soc.* **1976**, *98*, 8351. (b) McKenzie, T. C.; Sanner, R. D.; Bercaw, J. E. *J. Organomet. Chem.* **1975**, *102*, 457. (c) Lappert, M. F.; Martin, T. R.; Atwood, J. L.; Hunter, W. E. *J. Chem. Soc., Chem. Commun.* **1976**, 522. (d) Jeffrey, J.; Lappert, M. F.; Luong-Thi, N. T.; Webb, M.; Atwood, J. L.; Hunter, W. E. *J. Chem. Soc., Dalton Trans.* **1981**, 1593. (e) Fachinetti, G.; Fochi, G.; Floriani, C. *Ibid.* **1977**, 1946. (f) Hunter, W. E.; Atwood, J. L.; Fachinetti, G.; Floriani, C. *J. Organomet. Chem.* **1981**, *204*, 67.

(20) Atwood, J. L.; Hunter, W. E.; Hrncir, D. C.; Samiel, E.; Alt, H.; Rausch, M. D. *Inorg. Chem.* **1975**, *14*, 1757.

(21) Jeffrey, J.; Lappert, M. F.; Luong-Thi, N. T.; Atwood, J. L.; Hunter, W. E. *J. Chem. Soc., Chem. Commun.* **1978**, 1081.

Table II. Crystal and Intensity Collection Data for $Cp_2(PMe_3)Zr{=}CHO{-}Zr(I)Cp^*_2{\cdot}C_6H_6$

formula	$C_{34}H_{50}OPZr_2I{\cdot}C_6H_6$
formula weight	893.03
space group	$C2/c^a$
a, Å	27.318 (4)
b, Å	19.895 (3)
c, Å	19.932 (5)
β, deg	132.188 (10)
V, Å^3	8027 (3)
Z	8
D_{calcd}, g/cm^3	1.48
crystal size, mm	0.60 × 0.21 × 1.00
λ, Å	0.71069 (Mo Kα, graphite monochromator)
μ, mm^{-1}	1.338
2θ scan width, deg	1.0 below Kα_1, 1.0 above Kα_2
2θ limits (deg), scan rate (deg/min), bkgrd time/scan time, no. of reflns	3–35, 4.88, 1.0, 2599 ($+h,+k,\pm l$) 3–35, 8.37, 1.0, 2128 ($+h,+k,\pm l$) 35–46, 3.91, 1.0, 1960 ($+h,+k,\pm l$) 45–54, 2.02, 0.5, 5302 ($+h,+k,\pm l$) 3–30, 9.77, 1.0, 3501 ($+h,\pm k,\pm l$)
total no. of averaged data	8169 (7961)^b reflections
final no. of parameters	160
final agreement R_F	0.082 (7179)^c
R'_F	0.050 (4604)
R_{wF}	0.104 (7961)
S	1.74 (7961)

^{a} Data collected in $I2/a$: a = 19.932 (5) Å, b = 19.895 (3) Å, c = 20.303 (2) Å, β = 94.482 (9)°; all subsequent calculations carried out in $C2/c$. ^{b} 208 reflections deleted before final cycle of refinement; see text. ^{c} Number of reflections used in sums given in parentheses; see ref 37.

viewed along the Zr–C bond, the configuration of the carbene ligand is such that the proton and the zirconoxy substituents each eclipse a Cp ring, an arrangement that is required for Zr–C π-bonding of the carbon p-orbital and the $1a_1$ orbital in the zirconium equatorial plane. The data together with relatively short C–O (1.377 (9) Å[22]) and Zr(1)–O (1.940 (5) Å[23,24]) bond lengths suggest that all Lewis structures shown (I–IV) contribute to the

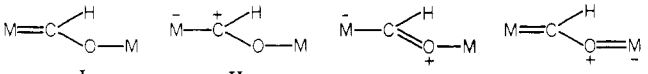

I II III IV

valence bond description of this compound. Treatment of $Cp_2(CO)Zr{=}CHO{-}Zr(H)Cp^*_2$ with CH_3I or $Cp_2(PMe_3)Zr{=}CHO{-}Zr(I)Cp^*_2$ with CO under carefully controlled conditions to avoid further reaction yields an intensely purple compound, $Cp^*_2ZrOCH{=}C(Zr(I)Cp_2)O$ (**8**). The ^{1}H NMR spectrum (Table I) shows signals for the C_5H_5 and C_5Me_5 rings and a resonance, integrating as one proton, at δ 6.8. The ^{13}C NMR spectrum of a sample prepared from $Cp_2(PMe_3)Zr{=}{}^{13}CHO{-}Zr(I)Cp^*_2$ (60% ^{13}C enriched) and ^{13}CO(99% ^{13}C enriched) shows two strong resonances downfield at δ 234.97 (99% ^{13}C enriched) and 155.01 (60% ^{13}C enriched) with $^1J_{CC}$ = 45 Hz and indicates that the carbene and carbonyl carbon atoms are coupled in the final product. The gated decoupled spectrum shows carbon–hydrogen coupling constants of $^1J_{CH}$ = 180 Hz and $^2J_{CH}$ = 24 Hz, values that are consistent with a new carbon–carbon bond. Treatment of unlabeled **7** with ^{13}CO gives incorporation of the labeled carbon atom only into the resonance at δ 235 with the small $^2J_{CH}$. The IR spectrum of a Nujol mull of **8** shows no evidence of any metal carbonyls.

The extensive rearrangement that is necessary to transform

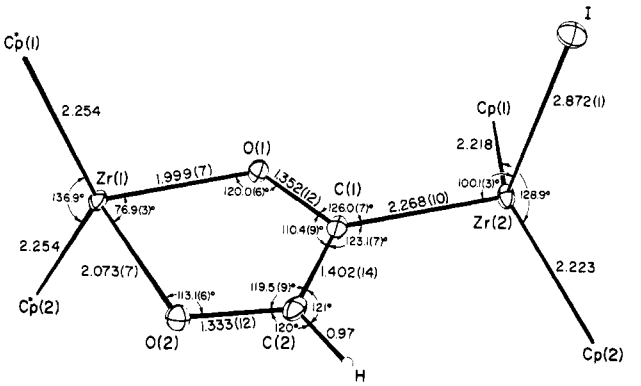

Figure 3. ORTEP drawing of **8** with important bond lengths and angles.

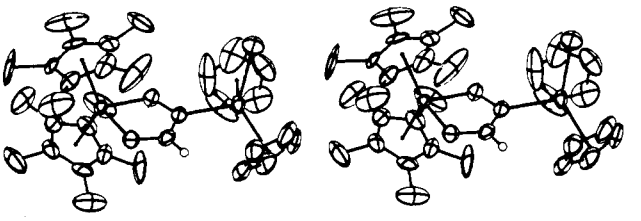

Figure 4. Stereoview of **8**.

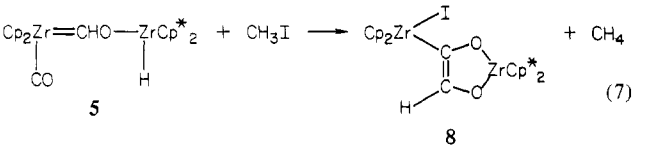

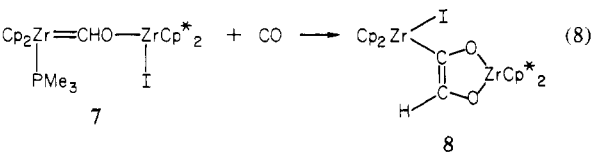

either of the starting carbene complexes to **8** made the assignment of its structure ambiguous from spectral data only. Hence suitable crystals for a single-crystal X-ray diffraction structure determination were grown by slow cooling of a saturated benzene solution. The unit cell parameters and a summary of data collection and refinement information are given in Table IV; atom coordinates are given in Table V.

The ORTEP drawing of **8** (Figure 3) confirms the formulation of the structure as a zirconium-substituted enediolate zirconocycle. Both zirconium atoms have pseudotetrahedral coordination geometries (Figure 4), and the metal-to-ring bonding for the Cp and Cp* ligands (Table XIII) is similar to that observed in the structure of **7**. The five-membered metallacycle ring is planar within experimental error (Table XV). The Zr(1)–O distances of 1.999 (7) and 2.073 (7) Å fall between those observed for zirconium acetylacetonate complexes[22] (2.10–2.25 Å: intermediate between covalent and dative Zr–O bond lengths) and zirconium μ-oxo dimers[23] (1.95 Å, covalent Zr–O bonding with significant π-bonding). The fact that the C–C bond length, 1.402 (14) Å, is slightly longer than that expected for a C–C double bond and that the C–O bonds (1.352 (12), 1.333 (12) Å) are shorter than the reported values for normal C–O single bonds[25] indicates that there is some π-delocalization throughout the metallacycle. The high-energy, empty zirconium orbital perpendicular to the bent metallocene equatorial plane, lone pair on the oxygen atom, and the C–C π-bond allows delocalization within the plane containing these seven atoms. The orientation of the $Cp_2Zr(I)$ fragment, with the Zr and I atoms in the metallacycle plane, suggests that

(22) Cardin, D. J.; Cetinkaya, B.; Lappert, M. F. *Chem. Rev.* **1972**, *72*, 575.

(23) (a) Silverton, J. V.; Hoard, J. L. *Inorg. Chem.* **1983**, *2*, 243. (b) Stezowski, J. J.; Eick, H. A. *J. Am. Chem. Soc.* **1969**, *91*, 2890. (c) Von Dreele, R. B.; Stezowski, J. J.; Fay, R. C. *Ibid.* **1971**, *93*, 2887. (d) Elder, M. *Inorg. Chem.* **1969**, *8*, 2103. (e) Chun, H. K.; Steffan, W. L.; Fay, R. C. *Ibid.* **1979**, *18*, 2458.

(24) (a) Clarke, J. F.; Drew, M. G. B. *Acta Crystallogr., Sect. B* **1974**, *B30*, 2267. (b) Petersen, J. L. *J. Organomet. Chem.* **1979**, *166*, 179.

(25) (a) Dunitz, J. D. "X-Ray Analysis and the Structure of Organic Molecules"; Cornell University Press: Ithaca, New York, 1979; p 338. (b) "International Distances, Supplement"; Sutton, L. E., Ed. *Spec. Publ.–Chem. Soc.* **1965**, *No. 18*.

Table III. Atom Coordinates ($\times 10^4$) for $Cp_2(PMe_3)Zr{=}CHO{-}Zr(I)Cp^*_2{\cdot}C_6H_6$

	x	y	z
I	3004.8 (2)	2451.9 (3)	3765.7 (3)
Zr(1)	3152.4 (3)	997.4 (3)	1334.7 (4)
Zr(2)	4246.9 (3)	2469.3 (3)	4187.4 (4)
P	3544.8 (8)	−231.5 (9)	2097.2 (12)
C(1)	4389 (4)	−464 (4)	2681 (5)
C(2)	3512 (4)	−394 (4)	2964 (5)
C(3)	3104 (4)	−957 (4)	1360 (5)
O	3968 (2)	1870 (2)	3217 (2)
C(4)	3895 (3)	1516 (3)	2564 (4)
C(11)	3525 (4)	421 (4)	597 (5)
C(12)	2963 (4)	785 (4)	−83 (5)
C(13)	3070 (4)	1464 (4)	93 (4)
C(14)	3730 (4)	1538 (4)	899 (5)
C(15)	4012 (3)	902 (4)	1221 (5)
C(21)	2196 (3)	611 (4)	1161 (6)
C(22)	2511 (3)	1117 (4)	1793 (5)
C(23)	2432 (3)	1722 (4)	1399 (5)
C(24)	2073 (3)	1603 (4)	479 (5)
C(25)	1926 (3)	905 (4)	320 (5)
C(31)	5167 (4)	2341 (3)	5962 (4)
C(32)	5402 (3)	2039 (4)	5579 (4)
C(33)	5007 (3)	1477 (3)	5079 (4)
C(34)	4525 (3)	1442 (3)	5136 (4)
C(35)	4615 (4)	1965 (3)	5673 (4)
C(41)	5541 (5)	2852 (4)	6725 (5)
C(42)	6053 (4)	2179 (5)	5829 (5)
C(43)	5118 (4)	978 (4)	4637 (5)
C(44)	4013 (4)	878 (4)	4730 (5)
C(45)	4291 (4)	2028 (5)	6051 (5)
C(51)	4706 (3)	3299 (3)	3761 (4)
C(52)	4007 (3)	3323 (3)	3011 (4)
C(53)	3719 (3)	3598 (3)	3323 (4)
C(54)	4225 (3)	3756 (3)	4244 (5)
C(55)	4843 (3)	3599 (3)	4518 (4)
C(61)	5201 (4)	3090 (4)	3694 (5)
C(62)	3660 (4)	3143 (4)	2048 (5)
C(63)	2996 (4)	3806 (4)	2696 (6)
C(64)	4134 (5)	4128 (4)	4819 (6)
C(65)	5506 (4)	3854 (4)	5339 (5)
C(71)	1454 (5)	959 (5)	3819 (7)
C(72)	987 (6)	479 (6)	3382 (8)
C(73)	855 (5)	97 (6)	2731 (7)
C(74)	1199 (5)	179 (5)	2470 (7)
C(75)	1708 (6)	643 (6)	2939 (8)
C(76)	1838 (5)	1047 (5)	3610 (7)
H(4)	4251 (27)	1547 (26)	2638 (35)

the metallacycle π-system delocalizes onto the Zr(2) center as shown by Lewis structure VI, although this orientation may be

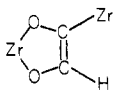

V

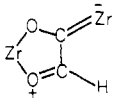

VI

due principally to Cp–Cp* nonbonded interactions. The Zr(2)–C bond length, 2.268 (10) Å, is indeed slightly shorter than the average observed for zirconium carbon single bond length[19,20] and is consistent with a limited π-interaction between these two atoms. The extended π-delocalization increases the C(2)–O(2) bond order while weakening the Zr–O(2) bond, relative to the corresponding bonds involving O(1), and thereby accounting for the different lengths of two Zr–O and two C–O bonds within the metallacycle.

The molecularity of the carbon–carbon bond forming step that leads to **8** was determined by a crossover experiment. Treatment of a mixture of $Cp_2Zr(^{12}CO)_2$ and $Cp_2Zr(^{13}CO)_2$ (91% ^{13}C enriched with $Cp^*_2ZrH_2$ followed by CH_3I yields **8** and **8**-$^{13}C_2$ with only 5 ± 5% isotopic scrambling, indicative of an intramolecular carbonyl–carbene coupling step.

These results suggest that the transformation of the carbene–carbonyl complexes to the insoluble yellow complex $(Cp_2Zr)(Cp^*_2ZrH)(C_2HO_2)$ (**6**), not seen for the carbene–phosphine compounds, might be initiated by coupling of the two ligands to

Table IV. Crystal and Intensity Data for $Cp^*_2\overline{ZrOCH{=}C(Zr(I)Cp_2)O}\cdot{}^1/_2C_6H_6$

formula	$C_{32}H_{41}IO_2Zr_2\cdot{}^1/_2C_6H_6$
formula weight	767.02
space group	$P2_1/c$
a, Å	15.866 (4)
b, Å	10.673 (3)
c, Å	20.561 (4)
β, deg	105.5 (2)
V, Å^3	3361 (1)
Z	4
D_{calcd}, g/cm^3	1.52
crystal size, mm	0.07 × 0.32 × 0.70
λ, Å	0.71069
μ, mm^{-1}	1.25
2θ scan width, deg	1.0 below $K\alpha_1$, 1.0 above $K\alpha_2$
refln settings	$(+h, +k, \pm l)$
2θ range (deg), scan rate (deg/min), and no. of reflns	$3 < 2\theta < 30$, 3.91 1250
	$30 < 2\theta < 45$, 2.02, 3450
backgrd time/scan time	1.00
total no. of averaged data	4100
final no. of parameters	361
final cycle[a] uncor, cor, limited	
R_F	0.096 (3891),[b] 0.074 (3922), 0.067 (2513)
R'_F	0.084 (3162), 0.059 (3069), 0.054 (1992)
S	4.44 (4100), 3.12 (4100), 2.93 (2691)

[a] Full data set, uncorrected for twinning used in refinement; full data set, corrected iteratively for twinning; limited data set, reflections affected by twinning deleted. [b] Number of reflections used in sums given in parentheses; see ref 37.

give a metal-bound ketene intermediate that oligomerizes or rearranges to give the isolated, insoluble product. The reactivity of **5** with Lewis bases is of interest, since these substrates are useful for stabilizing other group 4 metal ketene complexes are binding to the remaining coordination site on the metal,[26] thereby preventing oligomerization or further rearrangement. Indeed addition of ca. 4 equiv of pyridine to **5** in C_6D_6 affords a pyridine-trapped zirconium ketene complex, **9** rather than **6**, after 2 h at room temperature. **9** can be isolated in 82% yield by either dissolving

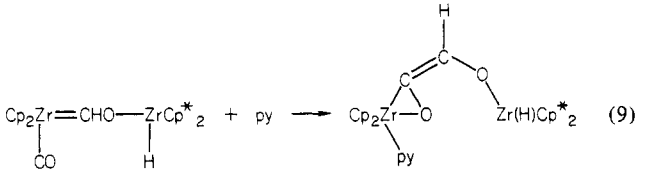

(9)

5 9

(py = pyridine)

4 in pyridine or treating $Cp_2Zr(CO)_2$ with $Cp^*_2ZrH_2$ in pyridine. The ^1H NMR spectrum of **9** (Table I) in C_5D_5N has single resonances for the Cp* and Cp rings at δ 2.18 and 5.91. No resonance can be assigned to the zirconium hydride in the 90-MHz spectrum; however, the 500-MHz spectrum has a small shoulder on the Cp peak at δ 5.92 in the region where the resonance for the hydride is expected. A peak integrating as one proton appears at δ 6.18 and is assigned as the resonance of the ketene hydrogen atom. This assignment is confirmed by the spectrum of **9** with the ketene carbon atoms enriched in ^{13}C. Treating $Cp_2Zr(^{13}CO)_2$ (70% ^{13}C-enriched) with $Cp^*_2ZrH_2$ in C_5D_5N yields **9**-$^{13}C_2$, for which the resonance at δ 6.18 is split by $^1J_{CH}$ and $^2J_{CH}$ of 183 and 22 Hz. The ^{13}C NMR spectrum (Table I) of the ^{13}C-enriched sample of **9** shows the ketene carbon atom resonances at δ 165.7 ($^2J_{CH}$ = 22 Hz) and 123.4 ($^1J_{CH}$ = 183 Hz) with $^1J_{CC}$ = 78 Hz and confirms that the product has a new carbon–carbon bond.

(26) (a) Straus, D. A. Ph.D. Thesis, California Institute of Technology, 1983. (b) Moore, E. J.; Straus, D. A.; Armantrout, J.; Santarsiero, B. D.; Grubbs, R. H.; Bercaw, J. E. *J. Am. Chem. Soc.* **1983**, *105*, 2068.

Table V. Atom Coordinates ($\times 10^4$) for $Cp^*_2\overline{ZrOCH{=}C(Zr(I)Cp_2)O}\cdot{}^1/_2C_6H_6$

	x	*y*	*z*
I	8334.0 (6)	4071.2 (8)	5237.7 (4)
Zr(1)	7311.8 (7)	5951.6 (8)	2294.2 (4)
Zr(2)	8038.7 (8)	2480.1 (9)	4073.6 (4)
O(1)	7928 (5)	4642 (6)	2941 (3)
O(2)	6311 (5)	5147 (6)	2628 (3)
C(1)	7468 (7)	3891 (9)	3252 (4)
C(2)	6583 (7)	4210 (9)	3061 (5)
C(11)	9588 (14)	2870 (15)	4255 (10)
C(12)	9326 (11)	2928 (20)	3601 (10)
C(13)	9034 (13)	1731 (24)	3375 (7)
C(14)	9216 (11)	1009 (13)	3947 (10)
C(15)	9586 (10)	1739 (16)	4493 (7)
C(21)	7026 (12)	1419 (13)	4682 (7)
C(22)	6522 (10)	2015 (11)	4138 (6)
C(23)	6586 (10)	1417 (10)	3545 (6)
C(24)	7210 (12)	492 (11)	3749 (7)
C(25)	7494 (12)	496 (12)	4466 (7)
C(31)	6765 (8)	8036 (9)	2625 (6)
C(32)	7419 (9)	8361 (8)	2317 (5)
C(33)	8238 (8)	7913 (9)	2678 (6)
C(34)	8079 (9)	7344 (9)	3269 (5)
C(35)	7197 (10)	7450 (10)	3220 (6)
C(31M)	5873 (12)	8335 (14)	2433 (10)
C(32M)	7292 (16)	9273 (11)	1722 (6)
C(33M)	9069 (11)	8092 (19)	2579 (11)
C(34M)	8763 (13)	6811 (13)	3831 (8)
C(35M)	6752 (17)	7032 (14)	3756 (9)
C(41)	6670 (9)	6052 (9)	1017 (5)
C(42)	7560 (9)	6085 (10)	1111 (5)
C(43)	7908 (8)	4936 (11)	1396 (5)
C(44)	7200 (9)	4204 (9)	1451 (5)
C(45)	6425 (9)	4879 (11)	1224 (5)
C(41M)	6011 (12)	7026 (13)	623 (7)
C(42M)	8077 (13)	7080 (14)	833 (6)
C(43M)	8813 (10)	4565 (19)	1556 (7)
C(44M)	7296 (14)	2852 (10)	1686 (6)
C(45M)	5537 (10)	4440 (17)	1162 (8)
C(3)	4305 (9)	−13 (12)	319 (6)
C(4)	5074 (10)	654 (11)	586 (6)
C(5)	5732 (9)	692 (11)	288 (6)

The ketene complex is stable for over a month at room temperature in pyridine solution. In benzene or toluene, however, **9** gives **6** (identified by IR), releasing pyridine, until an approximately fivefold excess of free pyridine to **9** is reached; complete conversion to **6** can be achieved by removing the pyridine in vacuo.

Treatment of **9** in C_5D_5N with 1 equiv of CH_3I in a sealed NMR tube affords a new complex, **10**, with ^1H and ^{13}C NMR spectra (Table I) similar to those of **9**. A small peak due to CH_4 is also seen in the spectrum of the reaction solution. On a preparative scale this reaction yields 0.88 equiv of CH_4, collected

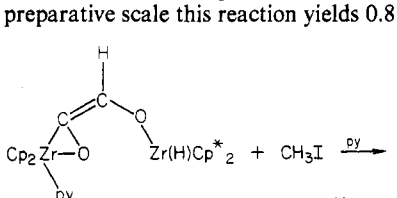

9

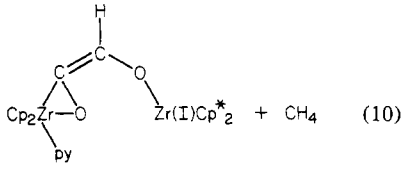

(10)

10

and measured with a Toepler pump, suggesting the formulation $Cp_2(py)Zr(O{=}C{=}CHO{-}Zr(I)Cp^*_2)$. Compound **10** has thus far been isolated only as an impure red tar. When the reaction of **9** and CH_3I is carried out in benzene or the isolated red tar is dissolved in C_6D_6, **8** is the major species observed by ^1H NMR. Conversely, **10** is the major species observed when **8** is dissolved in C_5D_5N. These results indicate that an equilibrium exists between **8** and **10**, with the predominant species dependent on pyridine concentration.

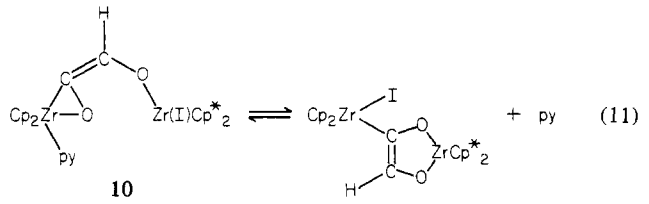

(11)

10 **8**

Other Lewis bases, such as phosphoranes, amines, or acetonitrile, are not effective for trapping of the zirconium ketene intermediate. Treatment of **5** with CH_2PMe_3 gives a complex mixture of unidentifiable products. NMe_3 is presumably too large to bind to the sterically hindered zirconium center and therefore does not prevent the conversion of **5** to **6**. In a manner similar to PMe_3, acetonitrile apparently displaces the remaining carbonyl to **4** to give a new carbene complex; however, this unstable intermediate has defied isolation. Unfortunately, hydrogenation of **9** under a vareity of conditions, in an attempt to obtain precedent for the final step of Scheme I, leads to a mixture of unidentifiable products.

Discussion

The general reaction shown in eq 1, the reduction of a transition-metal carbonyl by bis(pentamethylcyclopentadienyl)zirconium dihydride, has been extended to afford some of the first isolable examples of group 4 transition metal–carbon multiple bonding. The ready formation of **4** and **5** lends support to the proposed initial step of the mechanism for the formation of *cis*-$(Cp^*_2ZrH)_2(\mu\text{-}OCH{=}CHO{-})$ from $Cp^*_2Zr(CO)_2$ and $Cp^*_2ZrH_2$ under H_2 (Scheme I).[1d] The large difference in the rate of attack of $Cp^*_2ZrH_2$ on the Cp_2Zr carbonyls is very likely due to the increased steric hindrance of the bulky Cp* ligands. The zirconoxycarbene ligand lies between the two extremes: (i) Fischer-type carbene,[28] good σ-donor, poor π-acceptor interactions as in Lewis structures II and III (vide supra) and (ii) Schrock-type alkylidene, strong σ and π interactions[29,30] as in Lewis structure I. The $Cp^*_2(H)Zr^{IV}$ center is expected to compete with the carbene carbon atom for the oxygen lone pair as illustrated by Lewis structure IV. Thus the zirconoxycarbene should be a better π-acceptor than other Fischer-type, oxygen-stabilized carbenes. The strength of the Zr–C π bonding is apparent from the inequivalency of the two Cp resonances in the ^1H NMR spectra of **4**, **5**, and **7**, due to restricted rotation around the zirconium–carbene bond. The carbonyl stretching frequencies of some zirconocene carbonyl complexes provide additional insights on the electronic nature of the zirconoxy carbene ligand. The CO stretching frequency of **5** (1925 cm^{-1}) is very similar to the mean CO stretching frequency of **1** (1930 cm^{-1} from $\nu_{CO(sym)}$ = 1975 cm^{-1} and $\nu_{CO(asym)}$ = 1886 cm^{-1}),[31] suggesting that replacement of the carbonyl by zirconoxycarbene does not significantly change the electron density in the bent metallocene equatorial plane. By contrast, the ν_{CO} of **5** is much higher than that of **2** (ν_{CO} = 1852 cm^{-1}).[27] We conclude that the zirconoxycarbene is a good π-accepting ligand, comparable to CO in its π back-bonding with the zirconocene fragment. The carbon–hydrogen stretching frequency of the zirconoxycarbene C–H bond appears at relatively low energy in the IR spectra of **4**, **5**, and **7** (2755, 2755, 2725 cm^{-1}, respectively). It has been argued that distortion of the carbene ligand by lessening the metal–carbon–hydrogen angle parallels the lowering of ν_{CH}[32] and that both are measures of the carbon

(27) Demerseman, B.; Bouquet, G.; Bigorgne, M. *J. Organomet. Chem.* **1977**, *132*, 223.
(28) Brown, F. J. *Prog. Inorg. Chem.* **1980**, *27*, 1.
(29) (a) Schrock, R. R.; Sharp, P. R. *J. Am Chem. Soc.* **1978**, *100*, 2389. (b) Schrock, R. R. *Acc. Chem. Res.* **1979**, *12*, 98.
(30) Calabro, D. D.; Lichtenberger, D. L.; Herrmann, W. A. *J. Am. Chem. Soc.* **181**, *103*, 6852.
(31) Demerseman, B.; Bouquet, G.; Bigorgne, M. *J. Organomet. Chem.* **1976**, *107*, C19.

Scheme II

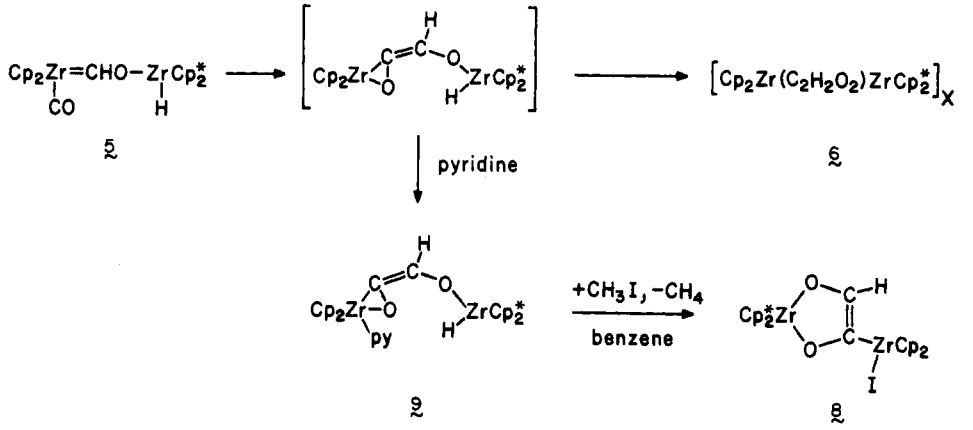

Scheme III

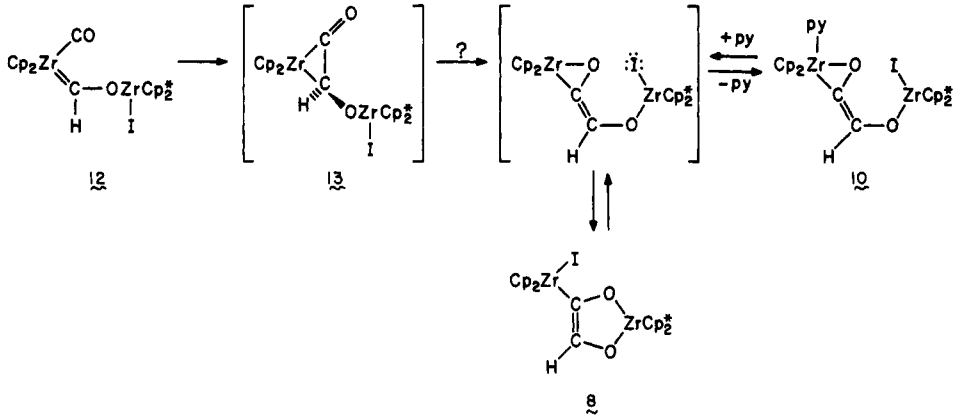

p character of the C–H bond, which should be increased in **4**, **5**, and **7** due to demand of the very electropositive zirconium for more carbon s character in the metal carbene σ bond.

The zirconoxycarbene–carbonyl complexes of zirconocene undergo facile rearrangement to a zirconium ketene intermediate by coupling these two equatorial ligands. In the case of **4** the ketene adduct, **11**, can be trapped by pyridine to afford the isolable zirconium ketene pyridine complex, **9**, as outlined in Scheme II. In the absence of a trapping ligand, **11** apparently isomerizes or oligomerizes to give **6**.

The replacement of the remaining zirconium hydride of $Cp_2(CO)Zr{=}CHO{-}Zr(H)Cp^*_2$ with an iodide, either by treatment of **5** with CH_3I or **7** with CO, results in the related carbonyl carbene complex **12**, which can couple to a new ketene adduct, **13** (Scheme III). Neither of these intermediates has been detected during the rearrangement to $Cp^*_2ZrO{-}CH{=}C(Zr(I)Cp_2)O$. We presume that the **13** to **8** process involves isomerization of the C,C-bonded to C,O-bonded ketene adduct followed by exchange of iodide and carbonyl oxygen between zirconium centers, the stability of the five-membered enediolate ring providing the driving force for the latter step. Although Cp and Cp* exchange cannot be ruled out by our data, we consider this a very unlikely alternative. Support for the ketene intermediate on the pathway to **8** is the observation of the pyridine adduct, **10**, obtained when the reactions that afford **8** in benzene are carried out in pyridine. Comparison of the ^{13}C NMR spectrum of **10** to those of **8** and **9** indicates that this compound is best formulated as a zirconium ketene complex with a structure similar to that of **9**.

The coupling of the carbene and carbonyl ligands is similar to the coupling of two carbenes to give an olefin complex, which has been recently discussed by Hoffmann and co-workers.[33] Their results indicate that the coupling is allowed for d^2 systems, so that ligand coupling also should be allowed for the d^2 zirconium carbene carbonyl complex.

Attempts to prepare $(Cp_2ZrH)(\mu\text{-}OCH{=}CHO{-})(Cp^*_2ZrH)$ by hydrogenation of **10**, analogous to the last step proposed in Scheme I, have been unsuccessful. While it could be argued that the presence of pyridine may slow the addition of H_2 to the Cp_2Zr center allowing other reaction pathways to become competitive, very similar Lewis base stabilized zirconium ketene complexes, $Cp^*_2(L)Zr(O{=}C{=}CHCMe_3)$ (L = py, CO, CH_2PMe_3), have been shown to hydrogenate cleanly to $Cp^*_2Zr(H)(OCH{=}CH(CH_2CMe_3))$, with a cis arrangement of the bulky substituents on the C=C bond.[26b]

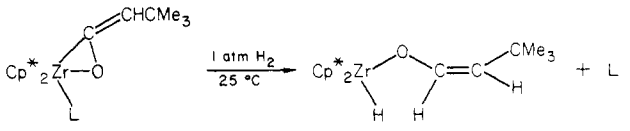

L = py, CO, CH_2PMe_3 (12)

Our results clearly provide support for the first three steps of Scheme I: (1) formation of a zirconoxy carbene carbonyl complex of zirconium, (2) intramolecular carbene carbonyl coupling, and (3) rearrangement of the initially formed C,C-η^2-ketene complex to the C,O-η^2-ketene form. While the final step has proved difficult to model with a zirconoxy species, eq 12 does speak to the viability of this step as well.

Experimental Section

General Considerations. All manipulations were performed under an inert atmosphere by employing a nitrogen-filled glovebox and vacuum line techniques. Hydrogen, nitrogen, and argon were purified by passing through MnO on vermiculite[34] and activated 4-Å molecular sieves. Benzene, toluene, and petroleum ether (30–60 °C), including NMR solvents, were vacuum transferred from $LiAlH_4$ or molecular sieves, then from "titanocene"[35] prior to use. Pyridine and methyl iodide were vac-

(32) Wood, C. D.; McLain, S. J.; Schrock, R. R. *J. Am. Chem. Soc.* **1979**, *101*, 3210.

(33) Hoffmann, R.; Wilker, C. N.; Eisenstein, O. *J. Am. Chem. Soc.* **1982**, *104*, 632.

uum transferred from CaH_2; pyridine-d_5 and acetone were transferred from 4-Å molecular sieves. Carbon monoxide (MCB), ^{13}C-carbon monoxide (Monsanto-Mound), and PMe_3 (Strem) were used as received.

$Cp_2Zr(CO)_2$,[31] $Cp_2Zr(CO)(PMe_3)$,[27] and $Cp^*_2ZrH_2$[1b] were prepared by literature methods. $Cp_2Zr(^{13}CO)_2$ was made by photolysis of $Cp_2Zr(CO)_2$ under a ^{13}CO atmosphere. $Cp^*_2ZrD_2$ was prepared by treatment of $[Cp^*_2ZrN_2]_2N_2$ with D_2 at low temperature and used promptly.

^1H NMR spectra were recorded by using C_6D_6, C_7D_8, or C_5D_5N as solvent with Me_4Si as an internal reference using Varian EM-390, JOEL FX90Q, and Bruker WM-500 spectrometers. ^{13}C NMR spectra were obtained with the JOEL instrument. IR spectra were recorded as Nujol mulls on a Beckmann IR 4240 spectrophotometer. Elemental analyses were performed by Alfred Bernhardt Analytical Laboratory and Dornis and Kolbe Microanalytical Laboratory.

Procedures. $Cp_2(PMe_3)Zr{=}CHO{-}Zr(H)Cp^*_2$ (4). at −196 °C 20 mL of toluene was added to a mixture of $Cp_2Zr(CO)(PMe_3)$ (1.30 g, 4.00 mmol) and $Cp^*_2ZrH_2$ (1.45 g, 4.00 mmol). The solution was stirred at −78 °C for 30 min to allow reaction and then warmed to room temperature. After filtration the solution was concentrated to 10 mL, and 15 mL of petroleum ether added to precipitate the red crystalline product. $Cp_2(PMe_3)Zr{=}CHO{-}Zr(H)Cp^*_2$ (2.30 g, 84%) was isolated by filtration and washed with cold petroleum ether. Anal. Calcd for $C_{34}H_{51}OPZr_2$: C, 59.25; H, 7.46; O, 2.32; P, 4.49; Zr, 26.47. Found: C, 58.69; H, 7.36; Zr, 26.79. IR (Nujol mull): 2755 w, 1560 w, 1280 w, 1100 s, 950 m, 775 m cm^{-1}.

$Cp_2(PMe_3)Zr{=}CDO{-}Zr(D)Cp^*_2$ was prepared in a similar manner using $Cp_2Zr(CO)(PMe_3)$ and $Cp^*_2ZrD_2$. IR (Nujol mull): 2045 vw, 1580 w, 1280 w, 1100 s, 950 m, 775 m cm^{-1}.

$Cp_2(CO)Zr{=}CHO{-}Zr(H)Cp^*_2$ (5). A petroleum ether solution of $Cp^*_2ZrH_2$ (250 mg, 0.69 mmol) was slowly added to a petroleum ether solution of $Cp_2Zr(CO)_2$ (210 mg, 0.76 mmol) at ca. −10 °C, resulting in an immediate color change from dark green to red. The solution was concentrated and cooled to −78 °C to precipitate the product as a tan solid. $Cp_2(CO)Zr{=}CHO{-}Zr(H)Cp^*_2$ (230 mg, 53%) was isolated by filtration at −78 °C, washed with cold petroleum ether, and dried in vacuo. Due to the instability of **5** in solution, recrystallization proved impossible. IR (Nujol mull): 2755 w, 1925 vs, 1620 w, 1515 w, 1170 s, 1155s, 1005 w, 780 m cm^{-1}.

$Cp_2(CO)Zr{=}CDO{-}Zr(D)Cp^*_2$ was prepared by using $Cp_2Zr(CO)_2$ and $Cp^*_2ZrD_2$. IR (Nujol mull): 2042 w, 1925 vs, 1570 w, 1170 s, 1155 s, 1005 w, 780 m cm^{-1}.

$[Cp_2Zr(C_2H_2O_2)ZrCp^*_2]_x$ (6). A mixture of $Cp_2Zr(CO)_2$ (190 mg, 0.69 mmol) and $Cp^*_2ZrH_2$ (250 mg, 0.69 mmol) was dissolved in 15 mL of benzene and stirred at room temperature for 10 h. The insoluble, yellow product precipitated from the reaction solution. **6** (115 mg, 25%) was isolated by filtration and washed with copious amounts of petroleum ether. Anal. Calcd for $C_{32}H_{42}O_2Zr_2$: C, 59.95; H, 6.60; O, 4.99; Zr, 28.46. Found: C, 59.82; H, 6.68. IR (Nujol mull): 1552 w, 1527 s, 1318 w, 1120 s, 1012 m, 967 w, 858 m, 794 s, 782 sh cm^{-1}.

$Cp_2(PMe_3)Zr{=}CHO{-}Zr(I)Cp^*_2$ (7). $Cp_2(PMe_3)Zr{=}CHO{-}Zr(H)Cp^*_2$ (1.50 g, 2.18 mmol) was dissolved in 30 mL of toluene. Methyl iodide (2.18 mmol), premeasured in a calibrated volume, was condensed into the reaction flask at −78 °C. The solution was stirred at room temperature for 30 min to effect reaction, indicated by a color change from red to green. The toluene was removed to yield the green crystalline product. $Cp_2(PMe_3)Zr{=}CHO{-}Zr(I)Cp^*_2$ (1.48 g, 83%) was washed with ca. 40 mL of petroleum ether at −78 °C and isolated by filtration. Anal. Calcd for $C_{34}H_{50}IOPZr_2$: C, 50.10; H, 6.18; I, 15.57; O, 1.96; P, 3.80; Zr, 22.38. Found: C, 49.84; H, 5.97; I, 15.86; P, 3.63. IR (Nujol mul): 2725 vw, 1280 w, 1075 s, 950 m, 780 m cm^{-1}. ^1H NMR spectrum of $Cp^*_2Zr(OCH_3)I$ obtained via eq 8: δ 1.86 (s, (η^5-C_5Me_5)), 3.67 (s, OCH_3) (benzene-d_6).

$Cp_2(PMe_3)Zr{=}CDO{-}Zr(I)Cp^*_2$ was prepared in a similar manner from $Cp_2(PMe_3)Zr{=}CDO{-}Zr(D)Cp^*_2$ and MeI. IR (Nujol mull): 2020 vw, 1280 w, 1075 s, 950 m, 780 m cm^{-1}.

$Cp^*_2\overline{ZrO{-}CH{=}C(Zr(I)Cp_2)O}$ (8). Toluene (25 mL) was condensed onto a mixture of $Cp_2Zr(CO)_2$ (0.83 g, 3.00 mmol) and $Cp^*_2ZrH_2$ (1.07 g, 3.00 mmol) at −196 °C and then warmed to 0 °C for ca. 5 min to effect formation of **5**. The reaction mixture was recooled to −196 °C and MeI (13 mmol) was added. When the reaction was stirred for 3.5 h at room temperature, the solution turned purple. On concentration of the toluene and addition of petroleum ether a dark purple solid was obtained $Cp^*_2\overline{ZrO{-}CH{=}C(Zr(I)Cp_2)O}$ (1.38 g, 60%) was recrystallized from benzene.

The above procedure was carried out by employing a mixture of $Cp_2Zr(CO)_2$ (73 mg, 0.263 mmol) and $Cp_2Zr(^{13}CO)_2$ (49 mg, 0.176 mmol) 91 ± 3% ^{13}C enriched). The ^{13}C NMR spectrum of the resulting product showed a ratio **8** (^{13}C, ^{13}C)/**8**(^{12}C,^{13}C) of 3.2 ± 0.4. When this number and the initial amounts of $Cp_2Zr(CO)_2$ and $Cp_2Zr(^{13}CO)_2$ are used, the calculated (no isotopic crossover) and actual **8**(^{12}C, ^{12}C):**8**(^{12}C, ^{13}C):**8**(^{13}C, ^{13}C) ratios from 59:8:33 and 58:10:32, corresponding to 5 ± 5% isotopic crossover on the formation of **8**.

In an alternative synthesis of **8**, a benzene solution of $Cp_2(PMe_3)Zr{=}CHO{-}Zr(I)Cp^*_2$ (710 mg, 0.87 mmol) was stirred under 200 torr CO for 3.5 h at room temperature. Longer reaction times or higher CO pressures led to a diminished yield of **8** due to further reaction. Removal of solvent and liberated PMe_3 in vacuo, washing with cold petroleum ether, and recrystallization from benzene to remove unreacted **7** gave $Cp^*_2\overline{ZrO{-}CH{=}C(Zr(I)Cp_2)O}$ in ca. 30% yield. Anal. Calcd for $C_{32}H_{41}IO_2Zr_2$: C, 50.11; H, 5.39; I, 16.55; O, 4.17; Zr, 23.79. Found: C, 50.34; H, 5.38; I, 16.38. IR (C_6D_6): 1433 m, 1380 w, 1250 m, 1120 w, 1020 w, 800 m cm^{-1}.

$Cp_2(py)Zr(O{=}C{=}CHO{-}Zr(H)Cp^*_2)$ (9). At −196 °C 15 mL of pyridine was condensed onto a mixture of $Cp_2Zr(CO)_2$ (425 mg, 1.53 mmol) and $Cp^*_2ZrH_2$ (550 mg, 1.52 mmol). The solution was stirred at room temperature for 1 h. Concentration of the solution to ca. 1 mL and addition of petroleum ether gave orange crystals. $Cp_2(py)Zr(O{=}C{=}CHO{-}Zr(H)Cp^*_2)$ (890 mg, 82%) was isolated by filtration, washed with cold petroleum ether, and dried in vacuo. Anal. Calcd for $C_{37}H_{47}NO_2Zr_2$: C, 61.68; H, 6.58; N, 1.95; O, 4.45; Zr, 25.34. Found: C, 61.73; H, 6.91; N, 1.96. IR (Nujol mull): 1600 m, 1518 w, 1216 w, 1110 s, 1008 m, 831 w, 788 s cm^{-1}.

$Cp_2(py)Zr(O{=}{}^{13}C{=}{}^{13}CHO{-}Zr(H)Cp^*_2)$ was prepared by using $Cp_2Zr(^{13}CO)_2$ (70% ^{13}C enriched) in place of $Cp_2Zr(CO)_2$ in the above procedure.

$Cp_2(py)Zr(O{=}C{=}CHO{-}Zr(I)Cp^*_2$ (10). CH_3I (0.061 mmol) was added to an NMR sample tube of **9** (40 mg, 0.056 mmol) in C_5D_5N at −196 °C, which was sealed. When the sample warmed to room temperature the ^1H NMR spectrum showed **10**. In a separate experiment CH_3I (0.134 mmol) was added to **9** (92 mg, 0.128 mmol) in pyridine at −196 °C and warmed to room temperature for 30 min; upon completion of the reaction 0.113 mmol of CH_4 (0.88 equiv of CH_4/equiv of **9**) were recovered by Toepler pump. A NMR sample of **9** (20 mg, 0.028 mmol) and CH_3I (0.14 mmol) in C_6D_6 gives a ^1H NMR spectrum identical with that obtained for **8** in C_6D_6 with 1 equiv of pyridine. Likewise, a sample of **8**, dissolved in C_5D_5N, has the same spectrum as **10** prepared from **9**.

Structure Determination of $Cp_2(PMe_3)Zr{=}CHO{-}Zr(I)Cp^*_2{\cdot}C_6H_6$. A large single crystal was mounted approximately along the *c*-axis in a glass capillary under N_2. A series of oscillation and Weissenberg photographs indicated monoclinic symmetry and a centered lattice, and the initial choice of axes conformed to $I2/a$ (hkl absent for $h + k + l$ odd, $h0l$ absent for h odd); data were collected on a locally modified Syntex $P2_1$ diffractometer with this unit cell. To be consistent with space group $C2/c$, the reflection indices were transformed for the subsequent calculations ($h' = h + l$, $l' = -h$). The lattice constants reported in Table II were obtained by least-squares refinement of 30 2θ values ($25 < 2\theta < 44°$), where each 2θ value was an average of two measurements at $\pm 2\theta$. The three check reflections indicated no decomposition and the data were reduced to F_0^2; the form factors for all atoms were taken from ref 36, and those for Zr and I were corrected for anomalous dispersion.

The positions of the Zr and I atoms were derived from the Patterson map, and the Fourier map phased on these three atoms revealed the remaining non-hydrogen atoms of the Zr complex. Least-squares refinement of atomic coordinates and U's, minimizing $\sum w[F_0^2 - (F_c/k)^2]^2$ gave $R_F = 0.131$.[37] A molecule of benzene and all hydrogen atoms were located from difference maps. The benzene molecule is apparently ordered and the coordinates of the carbon atoms were refined; all hydrogen atoms except H(4) were introduced into the model with fixed coordinates and isotropic B's. The refinement of all non-hydrogen atoms in the Zr complex with anisotropic U's, carbon atoms in the benzene molecule with isotropic B's, and the carbene hydrogen atom H(4) using all the data (8169 reflections) led to $R_F = 0.082$; the scale factor and Gaussian amplitudes in one block and the coordinates in the other. A number of reflections had large weighted residuals, and examination of the diffractometer data indicated that most of these reflections had unusual backgrounds or scans; these 208 reflections were deleted before the final cycle of refinement. All calculations were carried out on a VAX 11/780 using the CRYRM system of programs.

(34) Brown, T. L.; Dickerhof, D. W.; Bafus, D. A.; Morgan, G. L. *Rev. Sci. Instrum.* **1962**, *33*, 491.

(35) Marvich, R. H.; Brintzinger, H. H. *J Am. Chem. Soc.* **1971**, *93*, 2046.

(36) "International Tables for X-ray Crystallography"; Kynoch Press: Birmingham, England, 1974; Vol. IV, pp 72–98.

(37) $R_F = \sum||F_o| - |F_c||/\sum|F_o|$ sums include only those reflections with $F_o^2 > 0$. $R'_F = R_F$, but the sums include only those reflections with $F_o^2 > 3\sigma_{F^2}$. $S = \langle\sum w[(F_o^2 - (F_c/k)^2]^2/(n - v)\rangle^{1/2}$, where $w^{-1} = [s + r^2b + (0.02s)^2](k^2/Lp)^2$, n = total number of reflections, v = total number of parameters, s = scan counts, r = scan-to-background time ratio, b = background counts, k = scale factor, L = Lorentz factor and p = polarization factor.

Structure Determination for $Cp^*_2Zr(I)OCH=C(Zr(I)Cp_2)O\cdot{}^1/_2C_6H_6$. Single crystals were mounted in glass capillaries under H_2. Oscillation, Weissenberg, and precession photographs indicated a monoclinic lattice, space group $P2_1/c(0k0$ absent for k odd, $h0l$ absent for l odd), and twinning by reticular pseudomerohedry across the ab-plane with a twin index of 3: the $(h, k, (-l - 2h)/3)$ reflections of the twin lattice were superimposed onto the (h, k, l) reflections of the parent lattice. (The metric relation between a, c, and β is $3c (\cos \beta) = -a$.) The twin fraction varied with each crystal, indicating macroscopic twin domains. One of these crystals was selected for data collection on a locally modified Syntex $P2_1$ diffractometer. The three check reflections indicated no decomposition and the data were reduced to F_o^2.

The positions of the Zr and I atoms were derived from a Patterson map, and an electron Fourier map phased on these three atoms revealed the remaining non-hydrogen atoms of the Zr complex and a benzene molecule of crystallization. Least-squares refinement of atomic coordinates and U's minimizing $\sum w[F_o^2 - (F_c/k)^2]^2$ gave $R_F = 0.144$;[37] the form factors for all atoms were taken from ref 36. The hydrogen atoms were then located from difference maps and introduced into the model with fixed coordinates and isotropic B's. The refinement of non-hydrogen atoms with anisotropic U's using all the data (4100 reflections) led to $R_F = 0.096$, $R'_F = 0.084$, and $S = 4.44$.

At this stage, the F_o^2 were corrected for twinning in an iterative manner by substracting off an estimate of the twin contribution to the intensity.[38] This led to an improved data set, as evident from the lower goodness-of-fit: $S = 3.04$ ($R_F = 0.074$, $R'_F = 0.059$). After another cycle of least-squares refinement, the F_o^2 data were corrected again, but the correction differed marginally from the first pass: the volume ratio of the twins was 0.19:1; the final results are indicated in Table IV. The remaining errors in the data appear to be normally distributed. To check this, we carried out a parallel refinement in which all affected reflections were deleted. Refinement with this data set led to coordinates and U's that were insignificantly different (within 2σ) from the starting set; the goodness-of-fit (2.93, 2691 reflections total) is essentially the same as from the full data set refinement, and indicates that the twin correction is adequate ($R_F = 0.067$, $R'_F = 0.054$). All results quoted hereafter refer to refinement with the full data set.

(38) The twin fraction δ is defined by the relation $(kF_o)^2 = F_{cP} + \delta F_{cT}^2$, where k is the scale factor (estimated from the reflections unaffected by the twinning), F_o is the observed structure factor amplitude of the parent reflection, F_{cP} is the F_c of the parent reflection, and F_{cT} is the F_c of the twin reflection. The least-squares solution for δ gives $\delta = [k^2\sum wF_o^2F_{cT}^2 - \sum wF_{cP}^2F_{cT}^2]/\sum wF_{cT}^4$; the weight w is the least-squares weight for the twin reflection. The corrected F'_o is then calculated: $(kF'_o)^2 = (kF_o)^2 - \delta F_{cT}^2$ and used in the next cycle of least-squares refinement of coordinates and U's.

Acknowledgment. This work was supported by the National Science Foundation (Grant No. CHE 8024869). Use of the Bruker WM500 at the Southern California Regional NMR Facility, supported by National Science Foundation Grant No. CHE 7916324, is acknowledged. B.D.S. acknowledges support from the California Institute of Technology as a Myron A. Bantrell Fellow in Chemistry, 1981-1983.

Registry No. 1, 59487-85-3; **2**, 63637-45-6; **3**, 61396-34-7; **4**, 91202-93-6; **5**, 91202-95-8; **6**, 91208-76-3; **7**, 91202-97-0; **7**·C_6H_6, 91208-77-4; **8**, 91202-99-2; **8**·$^1/_2C_6H_6$, 91203-00-8; **8**-$^{13}C_2$, 91203-02-0; **8**-^{12}C,^{13}C, 91203-01-9; **9**, 91203-03-1; **9**-$^{13}C_2$, 91203-04-2; **10**, 91203-05-3; **12**, 91203-08-6; $Cp_2(PMe_3)Zr{=}CDO{-}Zr(D)Cp^*_2$, 91202-94-7; $Cp_2(CO)Zr{=}CDO{-}Zr(D)Cp^*_2$, 91202-96-9; $Cp_2(PMe_3)Zr{=}CDO{-}Zr(I)Cp^*_2$, 91202-98-1; $Cp^*_2ZrD_2$, 83708-61-6; $Cp^*_2Zr(OCH_3)I$, 91203-06-4; $Cp_2Zr(^{13}CO)_2$, 91203-07-5.

Supplementary Material Available: Tables of Gaussian amplitudes, H-atom coordinates, bond lengths and angles, least-squares planes, and listing of structure factor amplitudes for **7** and **8** (75 pages). Ordering information is given on any current masthead page.

Electronic Structure of Triple-Decker Sandwiches. Photoelectron Spectra and Molecular Orbital Calculations of Bis(η^5-cyclopentadienyl)(μ,η^6-benzene)divanadium and Bis(η^5-cyclopentadienyl)(μ,η^6-mesitylene)divanadium

Peter T. Chesky and Michael B. Hall*

Contribution from the Department of Chemistry, Texas A&M University, College Station, Texas 77843. *Received August 2, 1983*

Abstract: The first photoelectron spectra of triple-decker sandwich complexes are reported. The complexes $CpV(\mu,\eta^6\text{-}C_6H_6)VCp$ and $CpV(\mu,\eta^6\text{-}C_6H_3Me_3)VCp$ have only 26 valence electrons. Comparison of the experimental results with molecular orbital calculations shows that the ground states have four unpaired electrons. The order of the upper valence electrons differs from that predicted by earlier extended-Hückel calculations.

Molecular orbital calculations on triple-decker sandwich complexes such as [CpMCpMCp] and $[(CO)_3MCpM(CO)_3]$ (Cp = η^5-C_5H_5) predicted stable molecules for electron counts of 30 and 34.[1] A number of $M(CO)_3$ and MCp complexes with bridging heteronuclear ligands have been prepared.[2-7] Here, we report the first photoelectron (PE) spectra of triple-decker sandwich complexes. These complexes, $CpV(\mu,\eta^6\text{-}C_6H_6)VCp$ and $CpV(\mu,\eta^6\text{-}C_6H_3Me_3)VCp$,[8] have only 26 valence electrons. Comparison of the experimental results with molecular orbital (MO) calculations provides a definitive determination of the ground state and an assignment of the PE spectra.

Experimental Section

The complexes were kindly provided by Drs. K. Jonas and A. Duff (Max-Planck-Institut für Kohlenforschung, Mülheim, FDR). The spectra were recorded on a Perkin-Elmer PS-18 operating at a resolution of 35 meV for the Fwhm of the Ar $^2P_{3/2}$. Fenske-Hall MO calculations[9] were performed on the Department of Chemistry's VAX 11/780 with standard basis sets[10] and bond distances.[11]

(1) Lauher, J. W.; Elian, J.; Summerville, R. H.; Hoffmann, R. *J. Am. Chem. Soc.* **1976**, *98*, 3219.
(2) (a) Werner, H.; Salzer, A. *Synth. React. Inorg. Met.-Org. Chem.* **1972**, *2*, 239. (b) Salzer, A.; Werner, H. *Ibid.* **1972**, *2*, 249. (c) Salzer, A.; Werner, H. *Angew. Chem.* **1972**, *84*, 949.
(3) Beer, D. C.; Miller, V. R.; Sneddon, L. G.; Grimes, R. N.; Mathew, M.; Palenik, G. J. *J. Am. Chem. Soc.* **1973**, *95*, 3046.
(4) Herberich, G. E.; Hengesbach, J.; Kölle, U.; Huttner, G.; Frank, A. *Angew. Chem., Int. Ed. Engl.* **1976**, *15*, 433.
(5) Siebert, W.; Kinberger, K. *Angew. Chem., Int. Ed. Engl.* **1976**, *15*, 434.
(6) Edwin, J.; Bochmann, M.; Böhm, M. C.; Brennan, D. E.; Geiger, W. E.; Krüger, C.; Pebler, J.; Pritzkow, H.; Siebert, W.; Swiridoff, W.; Wadepohl, M.; Weiss, J.; Zenneck, U. *J. Am. Chem. Soc.* **1983**, *105*, 2582.
(7) Herberich, G. E.; Hessner, B.; Hultner, g.; Zsolnai, L. *Angew. Chem.* **1982**, *93*, 471.
(8) Duff, A. W.; Jonas, K.; Goddard, R.; Kraus, H.-J.; Krüger, C. *J. Am. Chem. Soc.* **1983**, *105*, 5479.
(9) Hall, M. B.; Fenske, R. F. *Inorg. Chem.* **1972**, *11*, 768.
(10) (a) Richardson, J. W.; Nieuwpoort, W. C.; Powell, R. R.; Edgell, W. F. *J. Chem. Phys.* **1962**, *44*, 1344. (b) Clementi, E. *Ibid.* **1964**, *40*, 1944. (c) Clementi, E. *IBM J. Res. Dev.* **1965**, *9*, 2.
(11) Distances used: Cp(centroid)-V = 1.90 Å, Bz(centroid)-V = 1.80 Å, V-C(Cp) = 2.23 Å, V-C(Bz) = 2.28 Å, C-C(Cp) = 1.38 Å, C-C(Bz) = 1.41 Å. These distances are reasonably close to those reported for the crystal structure.[8]

0002-7863/84/1506-5186$01.50/0